

Nanoscale

Accepted Manuscript



This is an *Accepted Manuscript*, which has been through the Royal Society of Chemistry peer review process and has been accepted for publication.

Accepted Manuscripts are published online shortly after acceptance, before technical editing, formatting and proof reading. Using this free service, authors can make their results available to the community, in citable form, before we publish the edited article. We will replace this *Accepted Manuscript* with the edited and formatted *Advance Article* as soon as it is available.

You can find more information about *Accepted Manuscripts* in the [Information for Authors](#).

Please note that technical editing may introduce minor changes to the text and/or graphics, which may alter content. The journal's standard [Terms & Conditions](#) and the [Ethical guidelines](#) still apply. In no event shall the Royal Society of Chemistry be held responsible for any errors or omissions in this *Accepted Manuscript* or any consequences arising from the use of any information it contains.

Multifunctional Role of Trialkylbenzene for the Preparation of Aqueous Colloidal Mesostructured/Mesoporous Silica Nanoparticles with Controlled Pore Size, Particle Diameter, and Morphology

Hironori Yamada,^{‡a} Hiroto Ujiie,^{‡a} Chihiro Urata,^a Eisuke Yamamoto,^a Yusuke Yamauchi,^b and Kazuyuki Kuroda^{*a,c}

^aDepartment of Applied Chemistry, Faculty of Science and Engineering, Waseda University, Ohkubo 3-4-1, Shinjuku-ku, Tokyo, 169-8555, Japan, ^bWorld Premier International (WPI) Research Center, International Center for Materials Nanoarchitectonics (MANA), National Institute for Materials Science (NIMS), 1-1 Namiki, Tsukuba, 305-0044, Japan, ^cKagami Memorial Research Institute for Material Science and Technology, Waseda University, Nishiwaseda 2-8-26, Shinjuku-ku, Tokyo, 169-0051, Japan

Fax: +81-3-5286-3199; Tel: +81-3-5286-3199; E-mail: kuroda@waseda.jp

‡ H. Yamada and H. Ujiie contributed equally.

Abstract

Both pore size and particle diameter of aqueous colloidal mesostructured/mesoporous silica nanoparticles (CMSS/CMPS) derived from tetrapropoxysilane were effectively and simply controlled by the addition of trialkylbenzenes (TAB). Aqueous highly dispersed CMPS with large pores were successfully obtained through removal of surfactants and TAB by a dialysis process. The pore size (from 4 nm to 8 nm) and particle diameter (from 50 nm to 380 nm) were more effectively enlarged by the addition of 1,3,5-triisopropylbenzene (TIPB) than 1,3,5-trimethylbenzene (TMB), and the enlargement did not cause the variation of the mesostructure and particle morphology. The larger molecular size and higher hydrophobicity of TIPB than TMB induce the incorporation of TIPB into micelles without the structural change. When TMB was used as TAB, the pore size of CMSS was also enlarged while the mesostructure and particle morphology were varied. Interestingly, when tetramethoxysilane and TIPB were used, CMSS with very small particle diameter (20 nm) with concave surfaces and large mesopores were obtained, which may strongly be related to the initial nucleation of CMSS. Judicious choice of TAB and Si sources is quite important to control the mesostructure, size of mesopores, particle diameter, and morphology.

Introduction

Mesoporous silica nanoparticles (MSN) are promising for various potential applications through effective use of designed mesopores by nanoscale downsizing of mesoporous silica having various characteristics, such as high surface area, high pore volume, tunable mesopores, easiness of surface modification, and mechanical and chemical stabilities.¹⁻¹⁸ MSN are expected to be applied in a wide variety of fields (adsorption, separation, drug delivery, and catalysis) because MSN have also colloidal characteristics, such as dispersity, transparency, and fluidity.¹⁹⁻³⁷ In addition, their properties and potentialities geared for applications have stimulated the development of the control in the composition, structure, and morphology of MSN.³⁸⁻⁴⁶

In particular, the control of pore size of MSN is quite important because it affects both the accessibility of in-coming guest molecules and the confinement effect of pores.⁴⁷⁻⁵⁴ The control of particle diameter of MSN has also a great significance in terms of the uptake, cytotoxicity, and dispersity of MSN.⁵⁵⁻⁶⁴ Thus, both control of pore size and particle diameter of MSN is largely meaningful for the precise preparation of different types of MSN appropriate to various applications.

It has already been known that pore size of mesoporous silica (including MSN) can be enlarged by adding a substance, like alkanes, alcohols, and trialkylbenzenes (TAB), into amphiphilic molecules or varying experimental conditions including the concentration of surfactants and the kinds of catalysts.^{46-51,63,65-75} One of the most frequently used expanders is TAB such as 1,3,5-triisopropylbenzene (TIPB) or 1,3,5-trimethylbenzene (TMB).⁷⁶⁻⁷⁸ TAB can enlarge pore size of MSN easily under a basic condition where it is easy to form MSN.^{47,50,75,79} Also, other particulate characteristics such as pore arrangement and particle diameter are varied by using TAB.^{47,50,75} Especially, it is quite reasonable to expect that the particle diameter of MSN can be enlarged by using the hydrophobicity of TAB. This is because the appropriate introduction of hydrophobicity in the reaction media can affect the hydrolysis rates of

alkoxysilanes, followed by the variation of dominance between nucleation and particle growth.⁸⁰ However, how the differences in the amount and kind of TAB affect pore size, pore arrangement, and particle diameter has not yet been clarified.

In this study, it has been clearly confirmed that how multifunctional role trialkylbenzene plays on pore size, particle diameter, and morphology of colloidal mesostructured and mesoporous silica nanoparticles (CMSS and CMPS, respectively) under a basic condition. (Please see Scheme 1.) As TAB, 1,3,5-triisopropylbenzene and 1,3,5-trimethylbenzene were used, and as Si sources, tetrapropoxysilane (TPOS) and tetramethoxysilane (TMOS) were used. When TIPB was used as TAB and TPOS as a Si source, both pore size (from 4 nm to 8 nm) and particle diameter (from 50 nm to 380 nm) were enlarged, depending on the amount of TIPB. When an excess amount of TMB was used as TAB, the pore size of CMPS was enlarged above 10 nm, but the mesostructure and particle morphology were varied. When TMOS and TIPB were used, CMPS with small particle diameter (20 nm), concave surface, and large pore (5-8 nm) were obtained, and they should be equivalent to particles at the initial nucleation. Thus, the kind of TAB played an important role in the enlargement of pore size and particle diameter of particles as well as in the variation of morphology. The differences in the mesostructure and particle diameter of CMSS by the kind of TAB should be ascribed to larger molecular size and higher hydrophobicity of TIPB than those of TMB, which indicates the different interactions between surfactant micelles and TAB. Moreover, removal of surfactants and TAB by a dialysis process was successfully achieved by modifying the dialysis process reported previously by us. These findings can provide a method to control both pore size and particle diameter of aqueous porous particles. This leads to the development of siliceous materials which can contain more and larger guest molecules and can reduce the nanorisks of toxicity toward applications for drug delivery, bioimaging, and catalysis.

Experimental Section

Materials.

Cetyltrimethylammonium bromide (CTAB) and triethanolamine (TEA) were purchased from Wako Pure Chem. Ind., Ltd. Tetramethoxysilane (TMOS : $\text{Si}(\text{OCH}_3)_4$), tetrapropoxysilane (TPOS : $\text{Si}(\text{OC}_3\text{H}_7)_4$), 1,3,5-trimethylbenzene (TMB) and 1,3,5-triisopropylbenzene (TIPB) were purchased from Tokyo Kasei Co., Ltd. Acetic acid (AcOH), ethanol (EtOH), and 2-propanol (2-PrOH) were purchased from Kanto Chem. Co., Inc. Sheet of high density polyethylene (HDPE) was purchased from PlaPort Co. Ltd. All substances were used without any further purification.

Characterization.

TEM images were taken on a JEOL JEM-2010 microscope operating at 200 kV. SEM images were taken on a HITACHI S-5500 electron microscope operated at an acceleration voltage of 5-30 kV. Samples for TEM and SEM measurements were dropped and dried on a carbon-coated micro-grid (Okenshoji Co.). X-ray diffraction (XRD) patterns of dried powder samples were obtained on a RIGAKU UltimaIV with Fe $K\alpha$ radiation (40 kV, 30 mA). Nitrogen gas adsorption-desorption measurements were performed with an Autosorb-2 instrument (Quantachrome Instruments) at -196 °C. Samples were preheated at 120 °C for 24 h under 1×10^{-2} Torr. Brunauer-Emmett-Teller (BET) surface areas were calculated from adsorption data in relative pressure range from 0.05 to 0.20. Pore volumes were calculated at $P/P_0 = 0.95$. Pore size distributions were evaluated using the adsorption branch with non-local density functional theory (NLDFT). Thermogravimetry-differential thermal analysis (TG-DTA) was carried out with a RIGAKU Thermo Plus 2 instrument under a dry air flow at a heating rate of 10 °C min^{-1} up to 900 °C. IR

1 spectra were obtained by using a JASCO FT/IR 6100 spectrometer by a KBr disk
2 method. Dynamic light scattering (DLS) measurements were conducted with a
3 HORIBA Nano Partica SZ-100-S at room temperature. The ζ -potential
4 measurements were conducted with an Otsuka Electronics ELSZ-1 at 20 °C.

5

6 **Preparation of Colloidal Mesoporous Silica Nanoparticles (CMSS) by** 7 **Adding Trialkylbenzene.**

8 (1) Preparation of CMSS without the addition of TAB.

9 According to previous reports,⁸⁰⁻⁸⁶ CMSS were prepared by tetraalkoxysilanes
10 (TPOS or TMOS). First, TEA (0.420 g), and CTAB (2.00 g) were added to 240 ml of
11 water (solution **1**). Next, the solution **1** (pH 9.5) was stirred at 80 °C for 2 h. Then 11
12 mmol of tetraalkoxysilanes (TPOS or TMOS) was added to the solution **1** and the
13 mixture was stirred vigorously at 80 °C for 12 h to become a colloidal state. Finally, the
14 colloidal suspension (pH 8.2) was filtered with a filtering paper (No. 5). The molar ratio
15 of the precursor solution was 1 tetraalkoxysilane : 0.50 CTAB : 0.25 TEA : 1200 H₂O.
16 The samples are denoted as P-as and M-as, corresponding to TPOS and TMOS,
17 respectively. The phrase “as” means “as-synthesized” or “before removal of
18 surfactants”.

19 (2) Preparation of CMSS by using TIPB and TPOS.

20 By varying the value of x which stands for the molar ratio of TIPB to CTAB,
21 CMSS were similarly prepared, as shown above (1). A certain amount of TIPB (5.5x
22 mmol: $x = 0.2, 0.4, 0.8, 2, 4, 8,$ and 20) were added to a precursor solution **1** (that is,
23 solution **2**), and the solution **2** was stirred for 30 min. Then, 11 mmol of TPOS was
24 added to the solution **2** and the mixture was stirred at 80 °C for 12 h to become a
25 colloidal state. Finally, the colloidal suspension was filtered with a filtering paper (No.
26 5). When the value of x was 0.8, an oil phase derived from TIPB was observed on the
27 surface of colloidal solution. With further increase in the value x , an oil phase was

1 observed on the surface of the main aqueous phase. A portion of oil phase was found on
2 the filtering paper on filtration for those cases. This means that the amount of TIPB in
3 the filtrates was not always same as the initial amount. The samples are denoted as
4 P_TIPB x -as.

5 (3) Preparation of CMSS by using TMB and TPOS.

6 Another type of CMSS was also prepared by using TMB as TAB, instead of
7 TIPB. The amount of TMB was 5.5 x mmol ($x = 0.8$ and 20). The samples are denoted as
8 P_TMB x -as.

9 (4) Preparation of CMSS by using TIPB and TMOS.

10 The other type of CMSS was similarly prepared by using TIPB as TAB and
11 TMOS as a Si source. The amount of TIPB was 4.4 mmol ($x = 0.8$) and that of TMOS
12 was 11 mmol. The sample is denoted as M_TIPB-as.

13

14 **Removal of Surfactants and TAB by a Dialysis Process.**

15 In order to remove surfactants and TAB, a dialysis process was conducted in
16 the same way as shown in our previous papers.^{80-82,84-87} A colloidal suspension (50
17 mL) of one of the following ones (P-as, M-as, P_TIPB x -as, P_TMB x -as, or
18 M_TIPB-as) was transferred into a dialysis membrane tube composed of cellulose
19 (molecular weight cut off = 12,000 – 14,000) and dialyzed for 12 h against 250 mL
20 of a mixture containing 2 M acetic acid and 2-propanol (1:1, v/v) and this process
21 was repeated five times. Then the tube, which contained CMPS, was immersed in
22 water to remove AcOH/2-PrOH in the tube, and the process was repeated twice.
23 Finally the pH value of the resulting solution was 3.4. The samples are denoted as
24 P-dia, M-dia, P_TIPB x -dia, P_TMB x -dia, or M_TIPB-dia, respectively, where “dia”
25 means “after dialysis” or “after removal of surfactants”. The removal of both
26 organics has been proved by the absence of IR peaks due to those organic

1 compounds and by no weight losses due to them, as shown in the TG curves
2 (Electronic Supplementary Information (ESI), Figures S1 and S2). In addition, dried
3 samples were obtained by heating a portion of CMPS at 120 °C for 12 h.

4 5 **Measurement of swelling ratios of HDPE for TMB and TIPB.**

6 In order to estimate the extent of affinity of TAB to alkyl chains of
7 surfactants, the swelling ratios of some fragments of HDPE sheet for TMB and TIPB
8 were measured. These ratios were obtained by comparing the initial volume with the
9 swollen volume after an immersion of HDPE fragments in TAB. Each piece was
10 immersed in 1 mL of TAB and shaken at 100 rpm for one week. After the procedure,
11 the pieces were dry-wiped to remove any residual liquid and weighed. Measurements
12 were performed at least 3 times for each sample. The details on the calculation of the
13 swelling ratios are shown in ESI.

14 15 **Results and Discussion**

16 **1. Preparation of CMSS and CMPS with Enlarged Pore Size and Particle** 17 **diameter by Adding TIPB.**

18 1.1 Characterization of P_TIPB_x-as.

19 All types of P_TIPB_x-as were somewhat transparent with clear Rayleigh and
20 Mie scatterings of the colloidal solutions without any aggregation, indicating their
21 high dispersity (Figure S3). As the amount of TIPB increased (*ie.* the increase in *x*),
22 the appearances of P_TIPB_x-as were more cloudy, suggesting that the particle
23 diameter became larger. As shown in the distributions of hydrodynamic diameters
24 measured by DLS (Figure S4), all types of P_TIPB_x-as show a single peak and no
25 peaks above 1000 nm are observed. On the basis of these data on the appearances
26 and particle size distributions, it was confirmed that the particle diameter of
27 P_TIPB_x-as increased with the amount of TIPB and that these CMSS were highly

1 dispersed. Also, the enlargement of particle diameter (from *ca.* 50 nm for P-as to *ca.*
2 380 nm for P_TIPB20-as) is shown in the TEM images (Figure S5). In terms of
3 mesostructure, the TEM images (Figure S5) show that the shape of mesostructure is
4 varied from worm-hole to radially-arranged, as the amount of TIPB increases. These
5 variations of particle diameter, pore size, and the shape of mesostructure (or pore)
6 will be discussed in the section 1.3.

7

8 1.2 Characterization of P_TIPB x -dia.

9 Removal of surfactants and TIPB by a dialysis process for P-as and
10 P_TIPB x -as was well accomplished with the retention of the dispersity of particles
11 (the details are shown in ESI). Like the cases of P_TIPB x -as, all types of
12 P_TIPB x -dia were almost transparent with clear Rayleigh and Mie scatterings of the
13 colloidal solution (Figure S6). Figure S7 shows that the particle diameter of
14 P_TIPB x -dia increased with the amount of TIPB and that these CMPS were highly
15 dispersed like the cases of the corresponding CMSS. As shown in Figures 1 and 2,
16 the enlarged particle diameter was retained.

17 On the basis of the TEM images (Figure 1), it was also confirmed that the
18 mesostructure was not varied after the dialysis. Mean pore size in each particle,
19 roughly estimated by the SEM images (Figure 2), was varied from *ca.* 4 nm to *ca.* 10
20 nm with the amount of TIPB, in the range of $x \leq 0.8$. The N₂ adsorption-desorption
21 isotherms (Figure S8) show type IV isotherms for all types of dried samples of
22 CMPS, meaning that they have mesopores. The relative pressure of capillary
23 condensation for P-dia is $P/P_0 = 0.4$, while in the cases of $x = 0.2, 0.4, 0.8$, and 2, the
24 values are $P/P_0 = 0.45, 0.5, 0.6$, and 0.65, respectively. Mean pore size of P-dia is
25 4.3 nm, while in the cases of $x = 0.2, 0.4, 0.8$, and 2, the pore size is enlarged to 4.9
26 nm, 6.6 nm, 7.0 nm, and 8.1 nm, respectively (Figure S8). In this range ($x \leq 2$), TIPB
27 should be incorporated into micelles of surfactants and micelles are sufficiently

1 swelled. On the other hand, in the range of $2 \leq x < 8$, the relative pressure is $P/P_0 =$
2 0.65 and mean pore size is 8.1 nm regardless of the amount of TIPB. This means that
3 the extent of swelling of micelles is limited. Moreover, in the case of $x = 20$, mean
4 pore size is 6.8 nm, smaller than those in the cases of $2 \leq x < 8$. The isotherm in this
5 case ($x = 20$) shows that the adsorbed amount of nitrogen is less than those of the
6 cases of other x values and that the shape of isotherm is different from others. The
7 excessive amount of TIPB should lead to the variation of the curvature and the shape
8 of micelles,⁸⁸ resulting in the transformation of structure.

9 The XRD patterns (Figure S9) show that the mesostructure is enlarged to
10 some extent with the amount of TIPB. In the region of $x \leq 2$, the periodicity of
11 structure is varied ($d =$ from 5.6 nm to 9.0 nm). In the region of $2 \leq x < 8$, the
12 variation of the periodicity of structure was not observed. However, in the case of x
13 $= 20$, the periodicity slightly decreased to 7.9 nm. The tendency will be discussed in
14 the next section.

15

16 1.3 Enlargement of both pore size and particle diameter of CMPS by adding TIPB.

17 The variations of pore size and particle diameter of CMPS with the amount
18 of TIPB are shown in Figure 3. The values of particle diameter were obtained from
19 the data in Figures S4 and S7, and the values of pore sizes were obtained from the
20 data in Figure S8. The overall tendency is divided into two parts. (i) In the range of 0
21 $\leq x \leq 8$, both the pore size and particle diameter are enlarged. While the pore size is
22 enlarged in the range of $0 \leq x \leq 2$ and becomes constant over $x = 2$, the particle
23 diameter is gradually and constantly enlarged in this range ($0 \leq x \leq 8$). (ii) In the
24 range of $8 < x \leq 20$, the pore size decreases and the particle diameter is obviously
25 enlarged. In this section, at first, the enlargement of particle diameter and pore size
26 by adding TIPB in the whole range is explained. Then, the roles of TIPB in the two
27 ranges described above are separately mentioned.

1 The general view about the enlargement of both pore size and particle
2 diameter is explained as follows. In terms of pore size, TIPB is incorporated into
3 micelles of surfactants, as reported previously.^{76-78,89-91} In terms of particle diameter,
4 the decrease of hydrolysis rate of alkoxy silanes leads to particle growth more
5 dominant than nucleation.^{80,82} In the present case, the interaction of TPOS with TIPB
6 due to hydrophobic interaction should inhibit the contact of TPOS with water. It
7 results in the decrease of hydrolysis rate of TPOS and then particle growth. After the
8 separate descriptions on the following two ranges (sections (i) and (ii)), the present
9 case is compared with the previously reported particle growth by the addition of
10 alcohols (section (iii)).⁸⁰

11 (i) $0 \leq x \leq 8$

12 Firstly, the enlargement of pore size with the increase in the molar ratio of
13 TIPB to CTAB (that is, the value 'x') is explained. As shown in Scheme 1, when x is
14 low ($x \leq 2$), TIPB molecules are probably located at the center of micelles of
15 surfactants. This means the swelling of micelles due to the incorporation of TIPB.
16 On the other hand, when x is larger ($2 < x \leq 8$), pore size is not enlarged. In this
17 region, the oil phase of TIPB in the resulting solution was obviously separated from
18 water. This means that, in the case of excess amount of TIPB, TIPB should be more
19 stable as a separated phase due to the aggregation of TIPB itself than as a solubilized
20 phase in micelles.

21 Next, the gradual enlargement of particle diameter is described as follows.
22 In particular, when x is low ($x \leq 2$), the enlargement was not clear, but when x is
23 larger ($2 < x \leq 8$), the enlargement is clearly shown. In the case of low x ($x \leq 2$), the
24 additional TIPB was mainly absorbed into micelles and it was unlikely for TIPB to
25 be separated from water and to contact with TPOS. In the case of higher x ($2 < x \leq 8$),
26 the phase separation of TIPB as an oil leads to the interaction with TPOS and the
27 lack of contact of TPOS with water. It causes the decrease of the hydrolysis rate of

1 TPOS as shown in Scheme 1, followed by particle growth more dominant than
2 nucleation. This phenomenon is similar to the previous study⁸⁰ in which the addition
3 of alcohols (typically butanol) leads to the decrease of the hydrolysis rates of
4 alkoxysilanes and the increase of the particle growth. Moreover, the enlargement of
5 particle diameter ($0 < x \leq 2$) compared to the particle diameter at $x = 0$ is due to a
6 slight interaction of TIPB with TPOS, although most of TIPB is absorbed into
7 micelles. This enlargement is also explained by the decrease of the hydrolysis rate of
8 TPOS.

9 Consequently, when x is low ($x \leq 2$), pore size is evidently enlarged due to
10 the incorporation of TIPB into micelles of surfactants, and the partial interaction of
11 TIPB with TPOS cause the decrease of hydrolysis rate of TPOS, leading to the slight
12 increase of particle diameter. When x becomes higher ($2 < x \leq 8$), pore size is not
13 enlarged because there is few space enough to incorporate TIPB into micelles. The
14 phase separation of TIPB from water and the increase of the interaction of TIPB with
15 TPOS leads to the obvious increase of particle diameter.

16 (ii) $8 < x \leq 20$

17 In the cases of $8 \leq x \leq 20$, the pore size of P_TIPB $_x$ -as decreased and
18 particle diameter clearly increased. Nitrogen adsorption-desorption isotherms
19 (Figure S8) show that the mesostructure changed. This variation should be due to the
20 relative large amount of oil (including TIPB) and also due to the formation of
21 complicated emulsion consisting of water, oil, and surfactants.⁹² In the present case,
22 the presence of excess amount of TIPB varied the structures of micelles, siliceous
23 species, and their composites, probably leading to the variation of mesostructure.
24 Thus, pore size was not enlarged and decreased in the range of $8 < x \leq 20$.

25 In addition, as x increased, the volume of oil increased and the amount of
26 TPOS incorporated into the oil phase also increased. As shown in Scheme 1, the
27 particle was grown successively to 380 nm.

1 (iii) Comparison of the present case with the case of the addition of propanol.

2 As reported previously,^{80,82} the decrease of hydrolysis rates of alkoxysilanes
3 leads to the enlargement of particle diameter. In the case of alcohols, it is necessary
4 to add 88 mmol of propanol (using TPOS) in order to enlarge particle diameter from
5 40 nm to 80 nm and to add 88 mmol of butanol (using TBOS) to enlarge from 80 nm
6 to 330 nm. On the other hand, in the case of TAB (in particular TIPB), 11 mmol of
7 TIPB can enlarge the particle diameter from 40 nm to 380 nm. That is, the effect of
8 TAB on the enlargement of particle diameter is much stronger than that of alcohol. It
9 should be ascribed to the lower relative electric permittivity (and thus higher
10 hydrophobicity) of TAB than that of butanol. (water: 80, TAB: 2 ~ 2.3, and butanol:
11 18) This means that TAB delays the hydrolysis of alkoxysilanes more effectively
12 than alcohols, followed by the particle growth more dominant than nucleation.

14 2. Preparation of CMSS and CMPS by Adding TMB.

15 2.1 Characterization of P_TMB_x-as and P_TMB_x-dia.

16 Like the cases of TIPB, the appearance of P_TMB_{0.8}-dia was almost
17 transparent with a slightly blue color, and with a clear Rayleigh scattering, as shown
18 in Figure S10b insets. From the DLS measurement of P_TMB_{0.8}-dia (Figure S11),
19 aggregates larger than 1000 nm in size were not observed and a single peak was
20 observed near 100 nm, which means nanoparticles are dispersed in an aqueous
21 medium. Nanoparticles with *ca.* 100 nm in size were also observed from the SEM
22 images (Figures S10b and S10f). In each case of $0 \leq x \leq 8$, the aqueous dispersity of
23 particles was confirmed (data not shown).

24 The SEM image of P_TMB_{0.8}-dia also shows that the pore size is *ca.* 4 nm
25 and that this value was similar to that of P-dia which were made without the addition
26 of trialkylbenzenes (Figures S10a and S10d). The N₂ adsorption-desorption
27 isotherms of the cases using TMB show that the values of P/P_0 corresponding to

1 capillary condensation are around 0.4 and that these are similar to that of P-dia
2 (Figure S12). Besides, in the cases of P_TMB x -dia ($0 \leq x \leq 0.8$), the pore sizes were
3 almost constant and independent of the values of x and the distinct enlargement of
4 pore size according to the increase of the value of x was not observed (Figure S13).
5 On the other hand, in the cases of P_TIPB x -dia ($0 \leq x \leq 0.8$), the relative pressures
6 (P/P_0) corresponding to capillary condensation were high (around 0.7), showing the
7 enlargement of pore size with the increase in the value of x .

8 The reason for the difference in the enlargement of pore size among various
9 kinds of trialkylbenzenes was discussed in the previous report by Fukuoka *et al.*⁹¹ It
10 is described that in the case of mesoporous silica made from CTAB micelles and
11 trialkylbenzenes, the position of trialkylbenzenes in micelles is a key factor for pore
12 size enlargement. On the basis of this report, the behavior of the formation of
13 micelles is described as follows. Because the structure of TMB is planar, a lot of
14 TMB molecules can get into the space between surfactant molecules in micelles
15 (Scheme 2b), thus micelles should not be enlarged clearly when the additional
16 amount of TMB increases. On the other hand, because the bulkiness of TIPB is
17 larger than that of TMB, lesser amounts of TIPB should exist in the spaces between
18 surfactants in micelles. Thus, it should be easy for TIPB to get into hydrophobic
19 central space of micelles (Scheme 2c). For this reason, the additional amount of
20 TIPB led to the increased accumulation in the hydrophobic center of micelles and the
21 distinct enlargement of micelles.

22 When the amount of TMB was increased ($x = 20$), radial mesopores were
23 observed from the TEM image and the size of mesopores was dozens of nanometers,
24 as shown in SEM image (Figure 4). The XRD pattern of the dried sample
25 (P_TMB20-dia) showed a very broad peak and a peak due to mesostructures was not
26 confirmed clearly (Figure S14). The reason for the formation of particles with large
27 radial mesopores will be discussed in the next section, on the basis of several

1 previous reports about particles with similar structures.

2

3 2.2 Effect of the kind of trialkylbenzene on the mesostructure and particle
4 morphology.

5 The differences in the mesostructure and particle morphology can be
6 explained by how TAB interacts with surfactants. On the basis of higher swelling
7 ratio of HDPE for TMB than that for TIPB (Table S1), TMB should be easier to
8 diffuse between alkyl chains of surfactants, while TIPB tends to assemble in the core
9 of micelles. (Scheme S2) Such a difference in the swelling behaviors will be used for
10 the discussion in the following paragraphs.

11 In order to obtain MSN with radial pores, typically shown in Figure 4, the
12 following two points are important, that is 1) suppression of the adsorption of
13 soluble silica species on the micelles of surfactants and 2) release of TAB
14 encapsulated in the micelles to vary the micelle-directed mesostructure. On the basis
15 of this consideration, besides, it has been reported that TMB can have cation- π
16 interaction with head groups of surfactants as well as hydrophobic interaction with
17 alkyl chains of surfactants.^{89,93} It was also reported that the cation- π interaction
18 becomes stronger in aqueous system.⁹⁴ Thus, in the present system, the phenomenon
19 1) must have occurred because the adsorption of soluble silica species on head
20 groups of surfactants is hindered due to the cation- π interaction between TMB and
21 surfactants. In the case of $x = 0.8$, particles with a disordered morphology were
22 obtained (Figure S10). This should be ascribed to the adsorption of TMB on micelles
23 in competition with soluble silica species, therefore, the contact points of silica
24 species with surfactants are heterogeneously limited. Moreover, in terms of the case
25 2), TMB should exist in the state as shown in Scheme 2b and TMB near the outer
26 surface of micelles can contact with solvents. In addition, TMB should be more
27 soluble gradually in the aqueous phase because the hydrophobicity of solvents

1 increases due to the presence of propanol generated from the hydrolysis of TPOS.
2 For these reasons, TMB can leak and diffuse from the inner space of micelles to the
3 outer (but still inside) space to make the shape of micelles larger along the axis of
4 rod-like micelles.

5 On the other hand, as shown in Scheme 2c, TIPB should exist in the inner
6 space of micelles and it is less likely for TIPB to contact with solvents in the outer
7 space of micelles. Thus, compared to the case of TMB, TIPB should be less affected
8 by the hydrophobization of solvents due to the presence of propanol (derived from
9 TPOS) and be less likely to leak and diffuse to the outside of micelles. It should lead
10 to the suppression of the formation of large radial pores as found for the case of
11 TMB. In addition, the steric hinderance of TIPB is larger than that of TMB, and thus
12 the cation- π interaction between head groups of surfactants and TIPB should be less
13 likely. On the basis of this consideration, it can be explained that spherical particles
14 were obtained in the case of $x = 0.8$ because the adsorption of soluble silica species
15 on micelles is thought to occur in a relatively homogeneous way. (Scheme 2b)

16 Moreover, it should be noted that the volume of TIPB is about twice larger
17 than that of TMB at the same molar concentration. This means TIPB can have
18 stronger effect on expanding the size of micelles than TMB, regardless of how TAB
19 interact with surfactants. However, in the present case, the expansion by TIPB (*ca.* 4
20 nm to 8 nm, in the range of $0 \leq x \leq 0.8$) occurred clearly, while the expansion by
21 TMB was not observed (almost the same *ca.* 4 nm, in the range of $0 \leq x \leq 0.8$). Thus,
22 it is shown that relative locations of TAB and micelles has a more great influence on
23 the expansion of pore size than the difference of volumes of TAB.

24 Consequently, the effects of the kind of TAB on the preparation of CMSS
25 and CMPS can be summarized in the following three points: (i) regardless of the
26 kind of TAB, colloidal mesoporous silica nanoparticles dispersed in aqueous
27 solution can be prepared, (ii) in the case of TIPB, pore size of CMPS can be

1 controlled easily with the amount of TIPB, and (iii) by varying the kind of TAB, the
2 mesostructures of CMSS and CMPS can be changed. These phenomena are
3 explained by the steric hinderance and hydrophobicity of TAB, that is, relative
4 locations of TAB and micelles. Such relations should affect the mesostructure as
5 well as the particle morphology of CMSS.

6 7 **3. Pore Size Enlargement of Colloidal Mesoporous Silica Nanoparticles with** 8 **Small Particle diameter.**

9 By using TIPB, the enlargement of pore size of small CMPS (20 nm) was
10 investigated. In terms of particle diameter, it was observed by SEM image (Figure 5)
11 that the particle diameters of both M-dia and M_TIPB-dia were about 20 nm
12 regardless of the presence of TIPB. Aggregates were not observed apparently.
13 However, as shown in particle size distributions measured by DLS (Figure 5), the
14 hydrodynamic diameter was about 40 nm and this means that secondary particles
15 were partly formed by the aggregation of primary particles.

16 It was confirmed by the N₂ adsorption-desorption isotherms (Figure S15)
17 that the pore size of M-dia, which was prepared without the addition of TIPB, was
18 about 4 nm. On the other hand, in the case of M_TIPB-dia, the pore size was about 5
19 nm. The degree of the enlargement for the cases of M-dia and M_TIPB-dia (from *ca.*
20 4 nm (M-dia) to *ca.* 5-8 nm (M_TIPB-dia)) is less than that of P-dia and
21 P_TIPB0.8-dia (from *ca.* 4 nm to *ca.* 7 nm). The state and composition of the
22 solution before the addition of Si sources is similar to those of P_TIPB0.8-as, and
23 the micelle size of M_TIPB-as should be about 7 nm. In view of the fact that the
24 particle diameter was about 20 nm, the size of micelles and pore size (*ca.* 5-8 nm)
25 are too large to form particles. Thus, all surfaces of micelles did not contribute to the
26 formation of the framework of particles but a part of surfaces contributed to form the
27 framework, leading to the formation of a silica nanostructure with a concave

1 surfaces.

2 The characteristics of silica nanostructure with concave surfaces is
3 explained as follows. In the step of the preparation of mesostructured silica
4 nanoparticles, the structure which consists of several micelles of surfactants,
5 corresponds to the structure in the initial step of nucleation. Taking account of the
6 mechanism proposed by Hollamby,⁹⁵ several species of silicate-surfactant composite
7 micelles are formed in the initial step of nucleation of mesostructured silica
8 nanoparticles. As shown in Scheme 3, the proposed model is applied to the present
9 case judging from the size of micelles and particle diameter of CMSS. This means
10 that the silica nanostructure with concave surfaces in this case is comparable to
11 particles in the initial step of nucleation. The present mesostructured and
12 mesoporous nanoparticles with concave surfaces had much smaller particle diameter
13 and the curvature of concaves was smaller than those reported previously on
14 MSN.^{81,95} These particles should contribute to the development of siliceous materials
15 which have both convex and concave surfaces for various applications of catalysis
16 and drug delivery.

17

18

Conclusion

19 Aqueous colloidal mesostructured silica nanoparticles (CMSS) were prepared by
20 varying the kind and amount of trialkylbenzenes (TAB) and by varying Si sources.
21 When 1,3,5-triisopropylbenzene (TIPB) was used as TAB and tetrapropoxysilane
22 (TPOS) was used as a Si source, both pore size (from 4 nm to 8 nm) and particle
23 diameter (from 50 nm to 380 nm) were enlarged with the amount of TIPB. In the case of
24 TPOS and an excess amount of 1,3,5-trimethylbenzene (TMB), the pore size of CMSS
25 was also enlarged above 10 nm, accompanied with the variation of mesostructure and
26 deformation of the spherical morphology. When tetramethoxysilane and TIPB were
27 used, CMSS with small particle diameter (20 nm), concave surfaces, and large pore (5-8

1 nm) were obtained, which should be equivalent to particles formed at the initial
2 nucleation. TIPB can enlarge pore size and particle diameter than TMB, and the
3 enlargement by TIPB was accomplished without the variation of mesostructure and
4 particle morphology. This should be ascribed to the larger size and higher
5 hydrophobicity of TIPB than those of TMB. Besides, removal of surfactants and TAB
6 by a dialysis process was successful for the preparation of aqueous highly dispersed
7 colloidal mesoporous silica nanoparticles with enlarged pores. The present findings will
8 lead to the development of siliceous materials which can accommodate more guest
9 molecules with larger size, and they can expand possible applications for drug delivery
10 and bioimaging as well as catalysis and concomitantly can reduce their nanorisks.

11

12 **Acknowledgement**

13 The authors thank Mr. M. Fuziwara (Waseda University) for his kind assistance
14 in TEM measurement. This work was supported in part by Grant-in-Aid for Scientific
15 Research, MEXT (15K13809).

16

1 **References**

- 2 (1) V. Valtchev and L. Tosheva, *Chem. Rev.*, 2013, **113**, 6734-6760.
- 3 (2) S.-H. Wu, C.-Y. Mou, and H.-P. Lin, *Chem. Soc. Rev.*, 2013, **42**, 3862-3875.
- 4 (3) C. E. Fowler, D. Khushalani, B. Lebeau, and S. Mann, *Adv. Mater.*, 2001, **13**,
5 649-652.
- 6 (4) S. Sadasivan, C. E. Fowler, D. Khushalani, and S. Mann, *Angew. Chem. Int. Ed.*,
7 2002, **41**, 2151-2153.
- 8 (5) H.-P. Lin and C.-P. Tsai, *Chem. Lett.*, 2003, 1092-1093.
- 9 (6) J. Fan, J. Lei, L. Wang, C. Yu, B. Tu, and D. Zhao, *Chem. Commun.*, 2003,
10 2140-2141.
- 11 (7) K. Suzuki, K. Ikari, and H. Imai, *J. Am. Chem. Soc.*, 2004, **126**, 462-463.
- 12 (8) K. Möller, J. Kobler, and T. Bein, *Adv. Funct. Mater.*, 2007, **17**, 605-612.
- 13 (9) J. Kobler and T. Bein, *ACS Nano*, 2008, **2**, 2324-2330.
- 14 (10) A. Berggren and A. E. C. Palmqvist, *J. Phys. Chem. C*, 2008, **112**, 732-737.
- 15 (11) F. Lu, S.-H. Wu, Y. Hung, and C.-Y. Mou, *Small*, 2009, **5**, 1408-1413.
- 16 (12) Y.-S. Lin, N. Abadeer, and C. L. Haynes, *Chem. Commun.*, 2011, **47**, 532-534.
- 17 (13) Y.-S. Lin, N. Abadeer, K. R. Hurley, and C. L. Haynes, *J. Am. Chem. Soc.*, 2011,
18 **133**, 20444-20457.
- 19 (14) K. Ma, H. Sai, and U. Wiesner, *J. Am. Chem. Soc.*, 2012, **134**, 13180-13183.
- 20 (15) K. Ma, U.-W. Zwanziger, J. Zwanziger, and U. Wiesner, *Chem. Mater.*, 2013, **25**,
21 677-691.
- 22 (16) D. Douroumis, I. Onyesom, M. Maniruzzaman, and J. Mitchell, *Crit. Rev.*
23 *Biotechnol.*, 2013, **33**, 229-245.
- 24 (17) M. Bouchoucha, R. C.-Gaudreault, M.-A. Fortin, and F. Kleitz, *Adv. Funct. Mater.*,
25 2014, **24**, 5911-5923.
- 26 (18) S. M. Egger, K. R. Hurley, A. Datt, G. Swindlehurst, and C. L. Haynes, *Chem.*
27 *Mater.*, 2015, **27**, 3193-3196.

- 1 (19) K. K. Unger, D. Kumar, M. Grün, G. Büchel, S. Lüdtke, T. Adam, K. Schumacher,
2 and S. J. Renker, *J. Chromatogr. A*, 2000, **892**, 47-55.
- 3 (20) S. H. Joo, J. Y. Park, C. K. Tsung, Y. Yamada, P. D. Yang, and G. A. Somorjai, *Nat.*
4 *Mater.*, 2009, **8**, 126-131.
- 5 (21) Y.-S. Lin, K. R. Hurley, and C. L. Haynes, *J. Phys. Chem. Lett.*, 2012, **3**, 364-374.
- 6 (22) K. C.-W. Wu and Y. Yamauchi, *J. Mater. Chem.*, 2012, **22**, 1251-1256.
- 7 (23) X. Li, J. C. Barnes, A. Bosoy, J. F. Stoddart, and J. I. Zink, *Chem. Soc. Rev.*, 2012,
8 **41**, 2590-2605.
- 9 (24) J. L. Vivero-Escoto, R. C. H. Phillips, and W. Lin, *Chem. Soc. Rev.*, 2012, **41**,
10 2673-2685.
- 11 (25) P. Yang, S. Gai, and J. Lin, *Chem. Soc. Rev.*, 2012, **41**, 3679-3698.
- 12 (26) P. Nadrah, O. Planinšek, and M. Gaberšček, *J. Mater. Sci.*, 2014, **49**, 481-495.
- 13 (27) X. Huang, N. P. Young, and H. E. Townley, *Nanomater. Nanotechnol.*, 2014, **4**,
14 1-15.
- 15 (28) L. Cheng, C. Wang, L. Feng, K. Yang, and Z. Liu, *Chem. Rev.*, 2014, **114**,
16 10869-10939.
- 17 (29) Y. Chen, H. Chen, and J. Shi, *Expert Opin. Drug Deliv.*, 2014, **11**, 917-930.
- 18 (30) P. Xu, S. Guo, H. Yu, and X. Li, *Small*, 2014, **10**, 2404-2412.
- 19 (31) X. Wang, H. Chen, K. Zhang, M. Ma, F. Li, D. Zeng, S. Zheng, Y. Chen, L. Jiang,
20 H. Xu, and J. Shi, *Small*, 2014, **10**, 1403-1411.
- 21 (32) R. Rogers, S. Kanvinde, S. Boonsith, and D. Oupický, *AAPS PharmSciTech.*,
22 2014, **15**, 1163-1171.
- 23 (33) I. Sierra, D. P.-Quintanilla, S. Morante, and J. Gañán, *J. Chromatogr. A*, 2014, **1363**,
24 27-40.
- 25 (34) S. A. Jadhav, *Inorg. Chem. Front.*, 2014, **1**, 735-739.
- 26 (35) C. Argyo, V. Weiss, C. Brauchle, and T. Bein, *Chem. Mater.*, 2014, **26**, 435-451.
- 27 (36) Y. Zhang, B. Y. W. Hsu, C. Ren, X. Li, and J. Wang, *Chem. Soc. Rev.*, 2015, **44**,

- 1 315-335.
- 2 (37) N. Song and Y.-W. Yang, *Chem. Soc. Rev.*, 2015, **44**, 3474-3504.
- 3 (38) M. Wang, Z. Sun, Q. Yue, J. Yang, X. Wang, Y. Deng, C. Yu, and D. Zhao, *J. Am.*
4 *Chem. Soc.*, 2014, **136**, 1884-1892.
- 5 (39) Q. Qu, G. Zhou, Y. Ding, S. Feng, and Z. Gu, *J. Non-Cryst. Solids*, 2014, **405**,
6 104-115.
- 7 (40) X. Du and S. Z. Qiao, *Small*, 2015, **11**, 392-413.
- 8 (41) X. Ma, K. Hahn, and S. Sanchez, *J. Am. Chem. Soc.*, 2015, **137**, 4976-4979.
- 9 (42) H. Ishii, T. Ikuno, A. Shimojima, and T. Okubo, *J. Colloid Interface Sci.*, 2015, **448**,
10 57-64.
- 11 (43) S. Rashi, S. K. Prajapati, and D. Singh, *World J. Pharma Pharm. Sci.*, 2015, **4**,
12 332-347.
- 13 (44) G. Chen, Z. Teng, X. Su, Y. Liu, and G. Lu, *J. Biomed. Nanotech.*, 2015, **11**, 1-8.
- 14 (45) Y. Chen, H. Chen, and J. Shi, *Adv. Healthcare Mater.*, 2015, **4**, 158-165.
- 15 (46) Z. Ma, J. Bai, Y. Wang, and X. Jiang, *ACS Appl. Mater. Interfaces*, 2014, **6**,
16 2431-2438.
- 17 (47) S. B. Hartono, M. Yu, W. Gu, J. Yang, E. Strounina, X. Wang, S. Qiao, and C. Yu,
18 *Nanotoxicology*, 2014, **25**, 1-12.
- 19 (48) D. Niu, Z. Liu, Y. Li, X. Luo, J. Zhang, J. Gong, and J. Shi, *Adv. Mater.*, 2014, **26**,
20 4947-4953.
- 21 (49) Z. Gao and I. Zharov, *Chem. Mater.*, 2014, **26**, 2030-2037.
- 22 (50) J. Peng, J. Liu, J. Liu, Y. Yang, C. Li, and Q. Yang, *J. Mater. Chem. A*, 2014, **2**,
23 8118-8125.
- 24 (51) L. Miller, G. Winter, B. Baur, B. Witulla, C. Solbach, S. Reske, and M. Lindén,
25 *Nanoscale*, 2014, **6**, 4928-4935.
- 26 (52) X. Ye, J. Wang, Y. Xu, L. Niu, Z. Fan, P. Gong, L. Ma, H. Wang, Z. Yang, and S.
27 Yang, *J. Appl. Polym. Sci.*, 2014, **131**, DOI: 10.1002/APP.41173.

- 1 (53) M. Wu, Q. Meng, Y. Chen, Y. Du, L. Zhang, Y. Li, L. Zhang, and J. Shi, *Adv.*
2 *Mater.*, 2015, **27**, 215-222.
- 3 (54) N. Ž. Knežević and J.-O. Durand, *Nanoscale*, 2015, **7**, 2199-2209.
- 4 (55) H. Vallhov, S. Gabrielsson, M. Strømme, A. Scheynius, and A. E. G. Bennett, *Nano*
5 *Lett.*, 2007, **7**, 3576-3582.
- 6 (56) D. Napierska, C. J. Thomassen, V. Rabolli, D. Lison, L. Gonzalez, M. K. Volders, J.
7 A. Martens, and P. H. Hoet, *Small*, 2009, **5**, 846-853.
- 8 (57) F. Lu, S.-H. Wu, Y. Hung, and C.-Y. Mou, *Small*, 2009, **5**, 1408-1413.
- 9 (58) Q. He, Z. Zhang, Y. Gao, J. Shi, and Y. Li, *Small*, 2009, **5**, 2722-2729.
- 10 (59) D. Napierska, L. C. J. Thomassen, D. Lison, J. Martens, and P. H. Hoet, *Part. Fibre*
11 *Toxicol.*, 2010, **7**, 39-70.
- 12 (60) V. Rabolli, L. C. J. Thomassen, C. Princen, D. Napierska, L. Gonzalez, M. K.
13 Volders, P. H. Hoet, F. Huaux, C. E. A. Kirschhock, J. A. Martens, and D. Lison,
14 *Nanotoxicology*, 2010, **4**, 307-318.
- 15 (61) Y.-S. Lin and C. L. Haynes, *J. Am. Chem. Soc.*, 2010, **132**, 4834-4842.
- 16 (62) F. Zhao, Y. Zhao, Y. Liu, X. Chang, C. Chen, and Y. Zhao, *Small*, 2011, **7**,
17 1322-1337.
- 18 (63) D. Shen, J. Yang, X. Li, L. Zhou, R. Zhang, W. Li, L. Chen, R. Wang, F. Zhang,
19 and D. Zhao, *Nano Lett.*, 2014, **14**, 923-932.
- 20 (64) M. Varache, I. Bezverkhyy, L. Saviot, F. Bouyer, F. Baras, and F. Bouyer, *J.*
21 *Non-Cryst. Solids*, 2015, **408**, 87-97.
- 22 (65) A. B. D. Nandiyanto, S.-G. Kim, F. Iskandar, and K. Okuyama, *Micropor. Mesopor.*
23 *Mater.*, 2009, **120**, 447-453.
- 24 (66) Y. Hoshikawa, H. Yabe, A. Nomura, T. Yamaki, A. Shimojima, and T. Okubo,
25 *Chem. Mater.*, 2010, **22**, 12-14.
- 26 (67) M.-H. Kim, H.-K. Na, Y.-K. Kim, S.-R. Ryoo, H. S. Cho, K. E. Lee, H. Jeon, R.
27 Ryoo, and D.-H. Min, *ACS Nano*, 2011, **5**, 3568-3576.
- 28 (68) V. Polshettiwar, D. Cha, X. Zhang, and J. M. Basset, *Angew. Chem. Int. Ed.*, 2010,

- 1 49, 9652-9656.
- 2 (69) S.-M. Lai, H.-Y. Lai, and M.-Y. Chou, *Microporous Mesoporous Mater.*, 2014, **196**,
3 31-40.
- 4 (70) Q. Cai, Z.-S. Luo, W.-Q. Pang, Y.-W. Fan, X.-H. Chen, and F.-Z. Cui, *Chem. Mater.*,
5 2001, **13**, 258-263.
- 6 (71) T. Yokoi, T. Karouji, S. Ohta, J. N. Kondo, and T. Tatsumi, *Chem. Mater.*, 2010, **22**,
7 3900-3908.
- 8 (72) J. Wang, A. S.-Narutaki, A. Shimojima, and T. Okubo, *J. Colloid Interface Sci.*,
9 2012, **385**, 41-47.
- 10 (73) K.-C. Kao and C.-Y. Mou, *Microporous Mesoporous Mater.*, 2013, **169**, 7-15.
- 11 (74) G. Sponchia, R. Marin, I. Freris, M. Marchiori, E. Moretti, L. Storaro, P. Canton, A.
12 Lausi, A. Benedetti, and P. Riello, *J. Nanopart. Res.*, 2014, **16**, 1-14.
- 13 (75) A. B. Fuertes, P. V.-Vigón, and M. Sevilla, *J. Colloid Interface Sci.*, 2010, **349**,
14 173-180.
- 15 (76) J. S. Beck, J. C. Vartuli, W. J. Roth, M. E. Leonowicz, C. T. Kresge, K. D. Schmitt,
16 C. T. W. Chu, D. H. Olson, E. W. Sheppard, S. B. McCullen, J. B. Higgins and J. L.
17 Schlenker, *J. Am. Chem. Soc.*, 1992, **114**, 10834-10843.
- 18 (77) N. Ulagappan and C. N. R. Rao, *Chem. Commun.*, 1996, **32**, 2759-2760.
- 19 (78) M. Luechinger, G. D. Pirngruber, B. Lindlar, P. Laggner, and R. Prins, *Micropor.*
20 *Mesopor. Mater.*, 2005, **79**, 41-52.
- 21 (79) Y. Zhang, H. Zhang, E. Che, L. Zhang, J. Han, Y. Yang, S. Wang, M. Zhang, and C.
22 Gao, *Colloids Surf., B*, 2015, **128**, 77-85.
- 23 (80) H. Yamada, C. Urata, H. Ujiie, Y. Yamauchi, and K. Kuroda, *Nanoscale*, 2013, **5**,
24 6145-6153.
- 25 (81) C. Urata, Y. Aoyama, A. Tonegawa, Y. Yamauchi, and K. Kuroda, *Chem. Commun.*,
26 2009, **45**, 5094-5096.
- 27 (82) H. Yamada, C. Urata, Y. Aoyama, S. Osada, Y. Yamauchi, and K. Kuroda, *Chem.*

- 1 *Mater.*, 2012, **24**, 1462-1471.
- 2 (83) H. Yamada, C. Urata, S. Higashitamori, Y. Aoyama, Y. Yamauchi, and K. Kuroda,
3 *ACS Appl. Mater. Interfaces*, 2014, **6**, 3491-3500.
- 4 (84) C. Urata, H. Yamada, R. Wakabayashi, Y. Aoyama, S. Hirose, S. Arai, S.
5 Takeoka, Y. Yamauchi, and K. Kuroda, *J. Am. Chem. Soc.*, 2011, **133**, 8102-8105.
- 6 (85) E. Yamamoto, M. Kitahara, T. Tsumura, and K. Kuroda, *Chem. Mater.*, 2014, **26**,
7 2927-2933.
- 8 (86) H. Ujiie, A. Shimojima, and K. Kuroda, *Chem. Commun.*, 2015, 51, 3211-3214.
- 9 (87) H. Yamada, C. Urata, E. Yamamoto, S. Higashitamori, Y. Yamauchi, and K. Kuroda,
10 *ChemNanoMat*, 2015, DOI: 10.1002/cnma.201500010.
- 11 (88) M. Tiemann, V. Goletto, R. Blum, F. Babonneau, H. Amenitsch, and M. Lindén,
12 *Langmuir*, 2002, **18**, 10053-10057.
- 13 (89) J. L. Blin and B. L. Su, *Langmuir*, 2002, **18**, 5303-5308.
- 14 (90) H. Kunieda, K. Ozawa, and K.L. Huang, *J. Phys. Chem. B*, 1998, **102**, 831-838.
- 15 (91) A. Fukuoka, I. Kikkawa, Y. Sasaki, A. Shimojima, and T. Okubo, *Langmuir*, 2009,
16 **25**, 10992-10997.
- 17 (92) D.-S. Moon and J.-K. Lee, *Langmuir*, 2012, **28**, 12341-12347.
- 18 (93) M. F. Ottaviani, A. Moscatelli, D. D.-Giscard, F. D. Renzo, P. J. Kooyman, B.
19 Alonso, and A. Galarneau, *J. Phys. Chem. B*, 2004, **108**, 12123-12129.
- 20 (94) J. P. Gallivan and D. A. Dougherty, *J. Am. Chem. Soc.*, 2000, **122**, 870-874.
- 21 (95) M. J. Hollamby, D. Borisova, P. Brown, J. Eastoe, I. Grillo, and D. Shchukin,
22 *Langmuir*, 2012, **28**, 4425-4433.

23

24

25

26

27

28

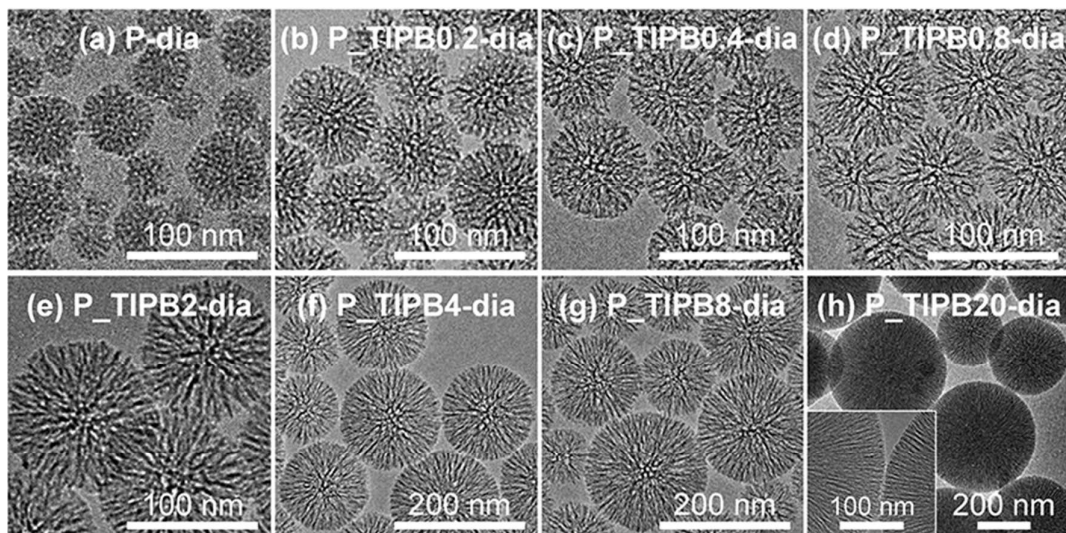
1
2
34
5
6
7
8
9

Figure 1 TEM images of P_TIPB x -dia: x = (a) 0, (b) 0.2, (c) 0.4, (d) 0.8, (e) 2, (f) 4, (g) 8, and (h) 20.

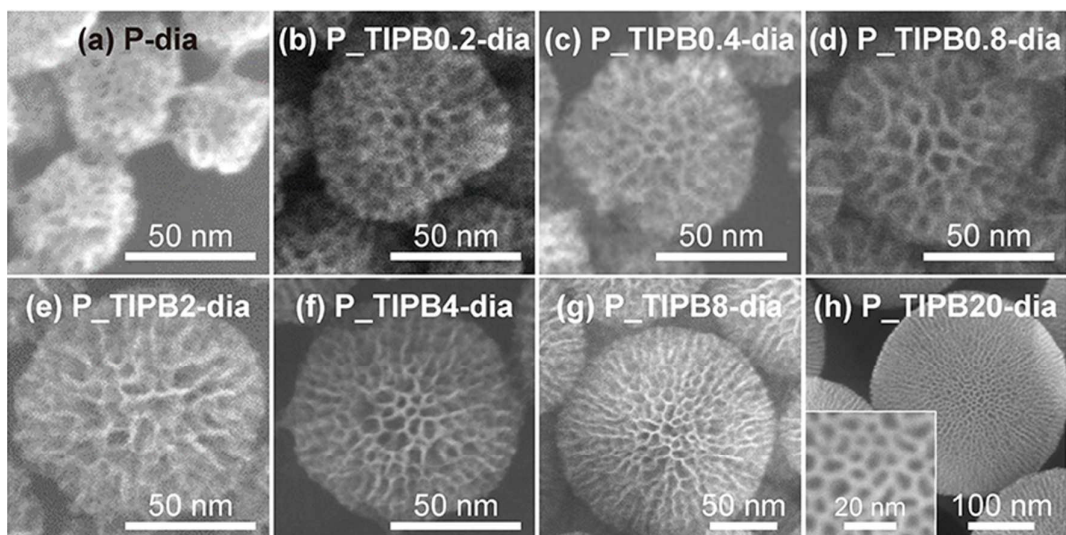
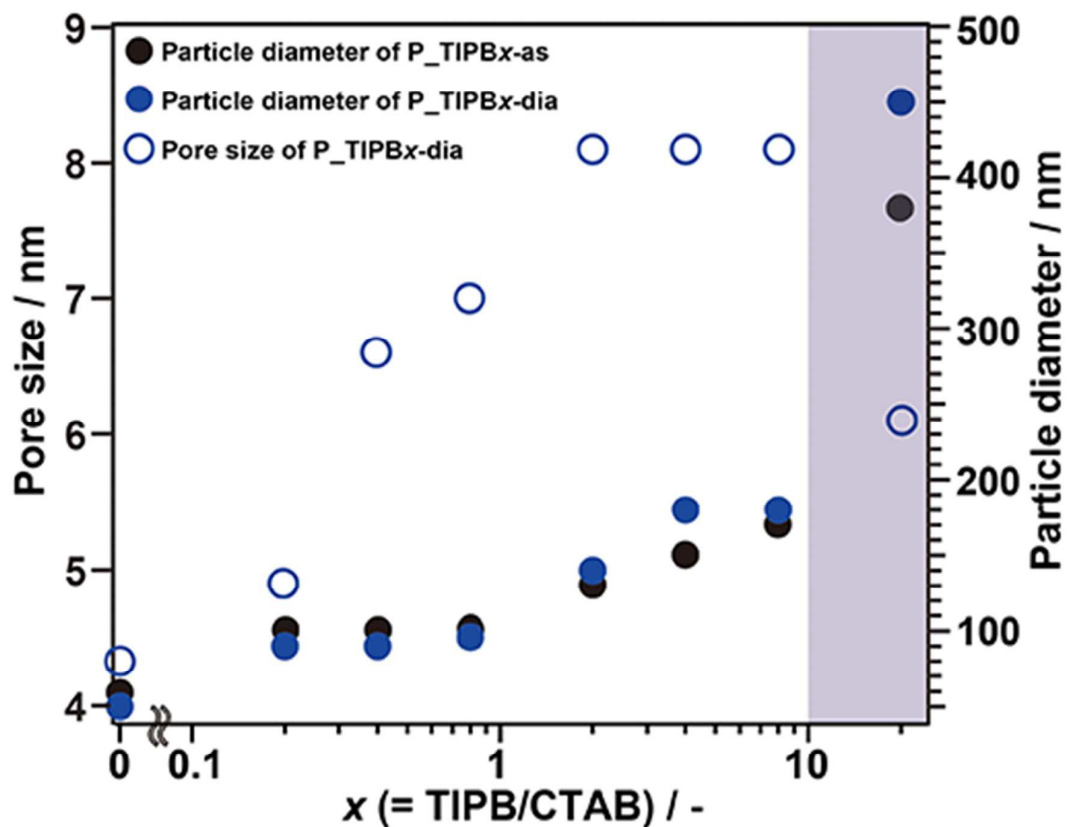
10
11
12
13
14
15

Figure 2 SEM images of P_TIPB x -dia: x = (a) 0, (b) 0.2, (c) 0.4, (d) 0.8, (e) 2, (f) 4, (g) 8, and (h) 20.

1
2
3
4
5
6
7
8
9



10
11
12
13
14
15
16

Figure 3 Variation of particle diameter and pore size of P_TIPBx-dia ($x = 0, 0.2, 0.4, 0.8, 2, 4, 8, \text{ and } 20$); Particle diameter was obtained from Figures S4 and S7, and pore size was obtained from Figure S8.

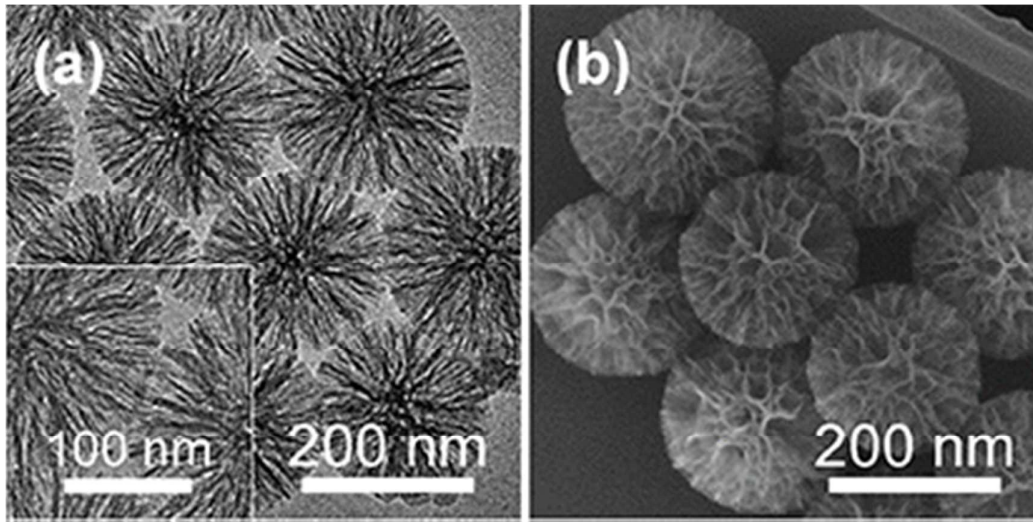


Figure 4 (a) TEM and (b) SEM images of P_TMB20-dia.

1
2
3
4
5
6
7
8

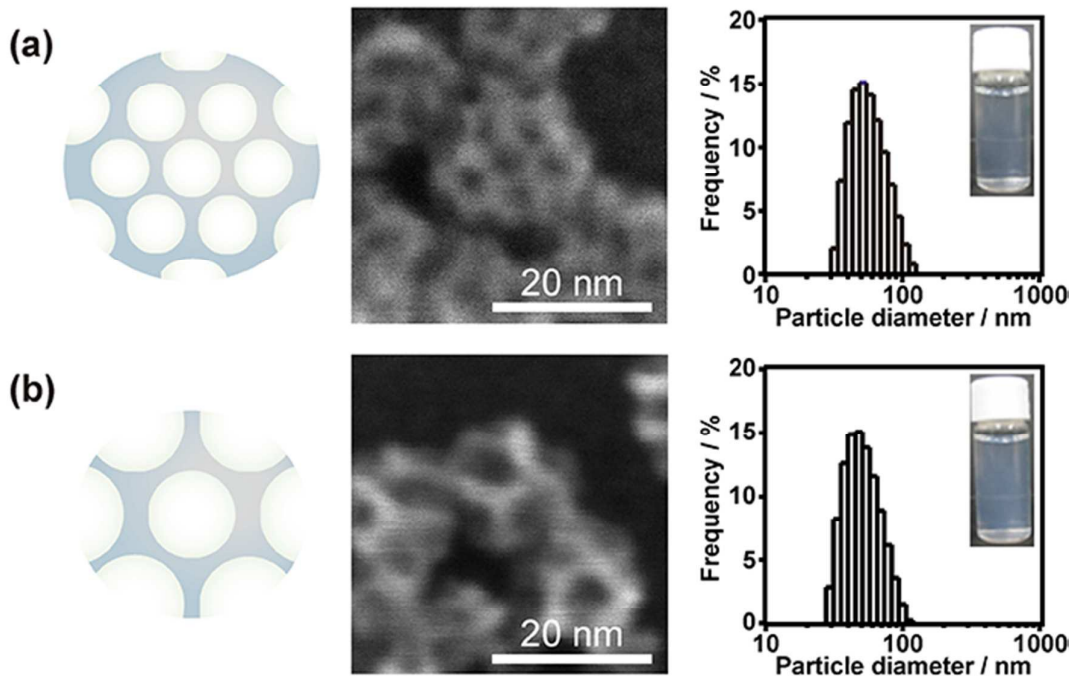
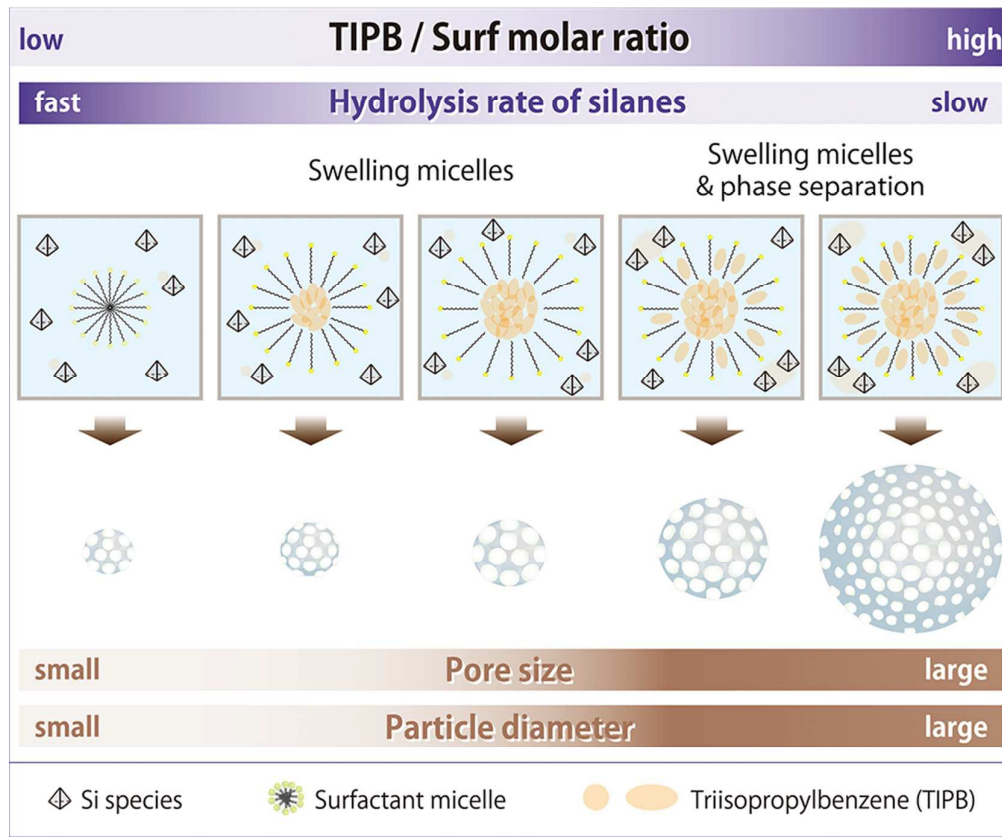
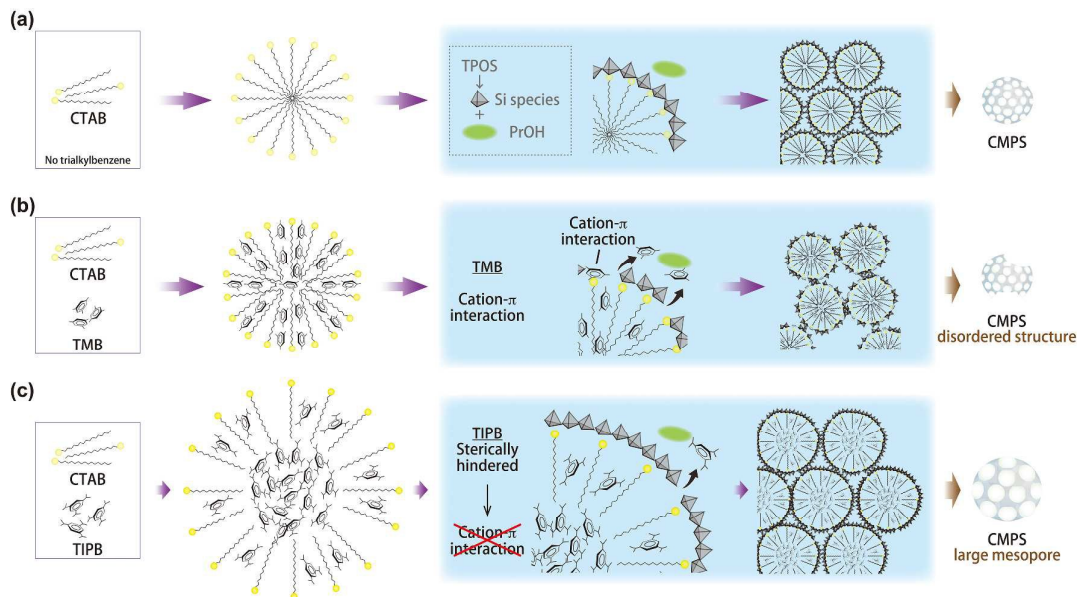


Figure 5 Schematic images, SEM images, appearances, and the particle size distributions (DLS, hydrodynamic diameter) of (a) M-dia and (b) M_TIPB-dia.

9
10
11



Scheme 1 Effect of TIPB on the preparation of CMSS.

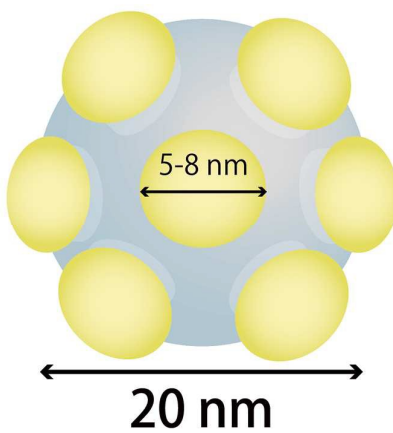


Scheme 2 Proposed structures of micelles and formation of CMPS; (a) without TAB, (b) with TMB, and (c) with TIPB.

1

2

3



4

5

Scheme 3 Proposed model of M_TIPB-as, which was prepared by using TIPB as TAB and using TMOS as a Si source.

6

7

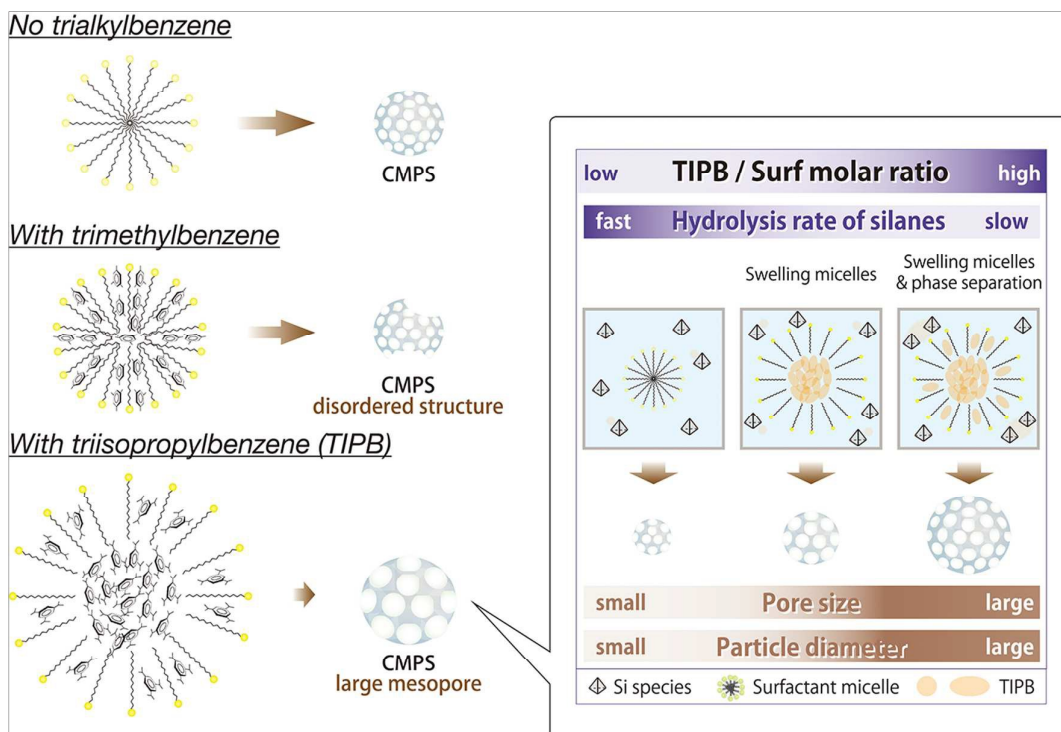
8

1 Table of Contents

2

3 Judicious choice of the amount and kind of trialkylbenzenes is critical to control pore
 4 size, particle diameter, and morphology of aqueous colloidal mesoporous silica
 5 nanoparticles.

6



7